The role of internal energy and approach geometry in molecule/surface reactive scattering

1995 J. Phys.: Condens. Matter 7 1023

(http://iopscience.iop.org/0953-8984/7/6/007)

J. Phys.. Condens. Matter 7 (1995) 1023–1045. Printed in the UK

REVIEW ARTICLE

The role of internal energy and approach geometry in molecule/surface reactive scattering

Dennis C Jacobs

Department of Chemistry and Biochemistry, University of Notre Dame, Notre Dame, IN 46556, USA

Received 10 November 1994

Abstract. The detailed mechanisms of many surface reactions are manifest through dynamical studies on well defined systems. In particular, the initial electronic, vibrational, and rotational energies, as well as the molecule's orientation and point of impact at the surface, are important in determining whether a molecule will react upon collision with a surface. These effects are delineated through state-resolved experiments involving various combinations of molecular beam, ion-beam, electrostatic field, laser excitation, and angle-resolved detection techniques. In conjunction with theoretical models, comprehensive surface-scattering experiments reveal the atomic motion that reactants undergo as they transform into scattered or adsorbed products.

1. Introduction

The interaction of molecules with surfaces has been a topic of vigorous research for some time. Originally, the motivation for surface science was born from a desire to understand and control heterogeneous catalysts in thermal reactors. The pursuant experimental studies were primarily focused on model reactions at metal surfaces under thermal conditions. Later the electronics revolution introduced a new applicability for surface science: that of semiconductor processing. Here, many commercial prescriptions for manufacturing electronic devices utilized reactive precursors (e.g., chemical vapour deposition) or high-energy particle collisions (e.g., ion implantation, ion sputtering, and reactive ion etching) to modify single-crystal semiconductor surfaces. More recently, environmental scientists have begun to explore the role of heterogeneous reactions in atmospheric processes; space scientists were intrigued with the array of hyperthermal energy collisions that low-earth-orbit spacecraft encounter in flight; and analytical chemists discovered that energetic ion/surface collisions could be exploited in tandem mass spectrometers for the purposes of chemical identification. In response to this growth in applications, the surface-science community has broadened its scope of topics and chemical environments to include a variety of related phenomena.

Two major goals pursued within surface science are the characterization of surface structures and the determination of mechanisms for surface chemical reactions. This review deals with the latter and borrows heavily from the approach of chemical reaction dynamics, a field that has evolved rapidly over the last three decades. Chemical reaction dynamics examines at a microscopic level the collective motion of atoms as reactants transform into products (see the book by Levine and Bernstein (1987)). An important distinction between studies in chemical kinetics and reaction dynamics is that the former treats a thermal system as progressing along a single ubiquitous reaction coordinate, whereas in the latter attention

0953-8984/95/061023+23$19.50

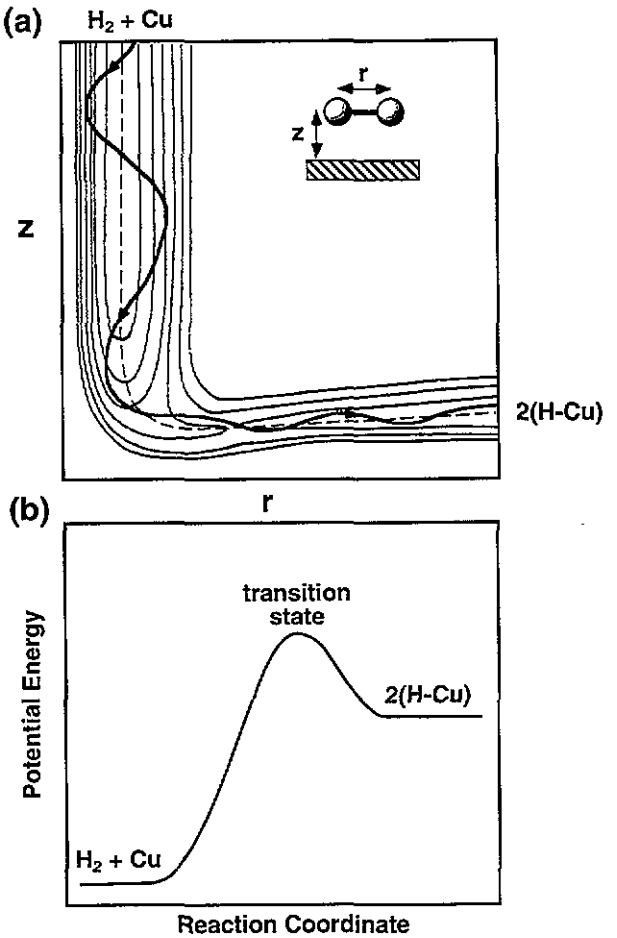

Figure 1. A comparison of potential-energy plots for H_2/Cu. (a) A multidimensional potential-energy surface retains the individual coordinates of the system (see the inset). The minimum-energy pathway is designated by a dashed curve. The solid curve represents a sample trajectory in which initial vibrational energy activates dissociative chemisorption. (b) The minimum-energy path is traced as the potential energy versus the reaction coordinate. (Adapted from the article by Darling and Holloway (1994)).

is given to motion along the various individual coordinates (bond lengths, angles, etc) as the reaction transpires. From a classical mechanical perspective, a surface reaction can be viewed as a system evolving on a multidimensional potential-energy hypersurface (figure 1(a)). A kineticist would simplify the problem by only exploring the minimum-energy path that leads from reactants to products on this hypersurface. This path could then be stretched out along one dimension, the reaction coordinate, against which the potential energy for the system is plotted (figure 1(b)). Extrema in this reduced-dimensionality plot would be associated with reactants, intermediates, transition states, or products. In contrast, a dynamicist attempts to retain the multidimensional character of the problem, so that vectorial information is not lost through averaging. For example, figure 2 illustrates a diatomic molecule approaching a rigid corrugated surface. In this simple planar representation, there

are four coordinates in the problem: z (the height of the molecule's centre of mass above the surface), r (the diatom's internuclear separation), θ (the orientation of the molecule's internuclear axis relative to the surface normal), and x (the point of impact at the surface). In a given classical trajectory, the path traversed along these four coordinates determines whether the molecule reacts, absorbs, or scatters. In reaction dynamics, experimentalists attempt to determine the extent to which different atomic motions influence the reaction probability for a given product channel.

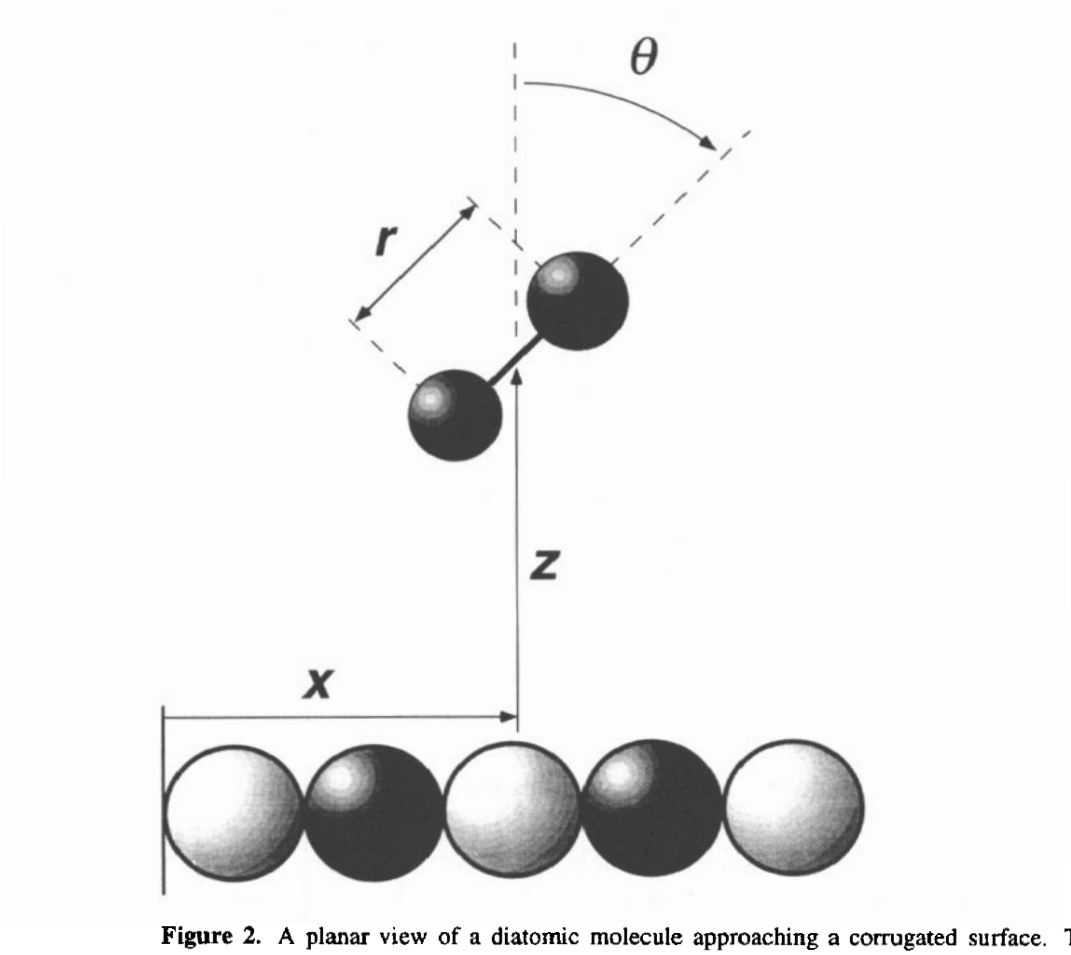

Figure 2. A planar view of a diatomic molecule approaching a corrugated surface. The four coordinates, z, r, θ and x, represent the height of the molecule's centre of mass above the surface, the diatom's internuclear separation, the orientation of the molecule's internuclear axis relative to the surface normal, and the point of impact at the surface, respectively. Experiments determine how the reaction probability depends on motion along these four coordinates by controlling the incident translational energy, the initial vibrational quanta, or the distribution of molecular orientations or by measuring the product scattering-angle/velocity distributions.

In many cases, one extracts dynamical information about a reactive process by using non-thermal distributions of reagents or by probing non-thermal distributions of products. It is convenient to categorize the initial conditions as being either energetic or geometric in nature. Translation, electronic, vibrational, and rotational energies each play an important role in activating the ensuing reaction. Approach geometry refers to the geometric or orientational configuration of the reagent molecule immediately prior to reaction on a surface. It includes both the position along the surface at which the molecule collides, i.e., surface impact parameter, and the alignment/orientation of the molecular axis relative to the surface plane. By controlling the distribution of energies and/or approach geometries

associated with the reagents, one can uniquely map the relationship between various initial conditions and their corresponding effects on reactivity. Similarly, by measuring the distribution of energies and geometries in the products, one learns the way in which a reactive system disposes of its energy and momentum. Together, these studies provide detailed information about a reaction mechanism, its transition state, and the specific motion along z, x, r and θ that underlies the nebulous reaction coordinate.

Two experimental tools have revolutionized the exploration of energy dependences in surface reactions: molecular-beam techniques and the use of lasers. Both neutral molecular beams and ion beams offer control over translational energy and feature a relatively small energy dispersion. Whereas supersonic expansions span an energy range from 10^{-2} to a few electronvolts, ion beams extend the range from a few electronvolts to many kiloelectronvolts. Internal energy (i.e., electronic, vibrational, and rotational) is often much lower than translational energy for these sources; however, it is usually difficult to vary the amount of internal energy over an appreciable range. This limitation can be overcome through the use of lasers, which precisely and selectively deposit molecular energy into internal degrees of freedom. In addition, lasers can probe the population of rovibronic sublevels associated with molecules leaving a surface.

Although the notion that reaction probability depends on approach geometry seems intuitive, experimental verification of these principles is difficult and rare. Inhomogeneous electrostatic fields or laser excitations have been instrumental in characterizing the effect of internuclear-axis orientation on surface reactivity. Collimated beams of reagents in conjunction with angle-resolved detection have illuminated the role of surface impact parameter in moderating surface reactivity.

This review will focus primarily on scattering experiments that assess the role of initial internal energy and/or approach geometry on the *reactivity* of molecules colliding with surfaces. The interested reader is referred to *DIET proceedings* (Tolk *et al* 1983, Brenig and Menzel 1985, Stulen and Knotek 1988, Betz and Vauga 1990, Burns *et al* 1993) for an overview of surface reactions initiated from photoexcited and electron-stimulated adsorbates. Although not covered here, these methods involve a restricted distribution of approach geometries over which hyperthermal energy reactions can be explored. Moreover, previous reviews on molecule/surface scattering have addressed the effect of incident translational energy on surface reactivity (see the article by Ceyer (1988)). Figure 3 lists a series of fundamental molecule/surface processes and shows the approximate collision-energy range over which these processes are studied. Although collision energy is usually the dominant factor in determining reaction probability upon impact, it is certainly not the sole factor. Non-unit reaction probabilities for systems at energies above the activation barrier underscore the importance of approach geometry and internal energy in any complete dynamical picture.

2. Internal energy

An essential issue regarding the investigation of internal-energy dependences for surface reactions is whether an initial distribution of excited states completely relaxes before the molecule reaches the transition-state region. The concern can be validated or dismissed through a simple comparison of the molecule/surface interaction time with the lifetime of an excited molecular state near the surface. A molecular electronic state usually couples strongly to near-resonant, evanescent bulk and surface states; consequently, the excited-state energy level broadens. Near metallic and semiconducting surfaces, electronically-excited-state lifetimes are typically of the order of 10^{-15}–10^{-14} s. Vibrationally excited states

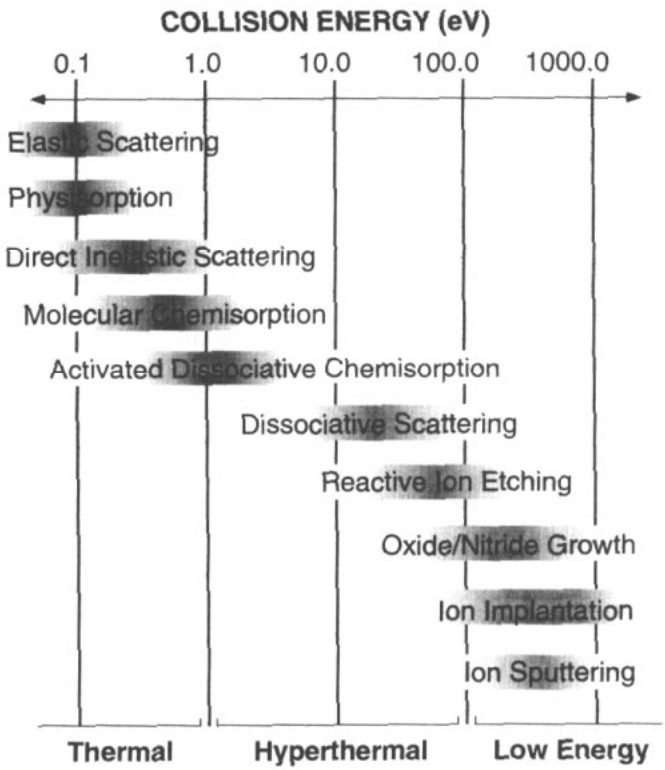

Figure 3. Fundamental molecule/surface processes. Each shaded region designates the energy range over which the associated process is studied.

do not couple as strongly. Lifetime measurements reveal that a quantum of vibrational excitation within an adsorbate lives for $\sim 10^{-12}$ s, 10^{-9} s, or 10^{-3} s near metallic, semiconducting, or insulating surfaces, respectively (see the article by Cavanagh *et al* (1994)). Rotational energy is damped through mechanical means within the bounds of momentum conservation. This can often occur over a few rotational periods (10^{-12}–10^{-11} s). As a point of comparison, the interaction time for a direct molecule/surface collision can be estimated from the molecule's incident velocity. For example, a typical small molecule (30 amu) travels 1 Å in 2×10^{-13} s at room temperature, 1 Å in 4×10^{-14} s at 1 eV, and 1 Å in 6×10^{-15} s at 50 eV. With the exception of electronically excited states, internal excitations within incident molecules should not be completely quenched during a single surface collision. In the following three subsections, experimental efforts that ascertain the individual roles of initial electronic, vibrational, and rotational energy, respectively, in reactive collisions are reviewed.

2.1. Electronic energy

The relatively short lifetime of electronically excited states is problematic when trying to experimentally determine the effect of electronic excitation on reactive scattering. Often, a laser must be directed at the surface during molecular-beam exposure in order to insure sufficient electronic excitation. Unfortunately, this optical configuration allows for photoexcitation of not only impinging gas-phase molecules, but also surface adsorbates and

the solid substrate. As a result, ambiguities arise as to the nature of an observed photo-enhanced reactivity. Nevertheless, lasers have been used to generate radicals through the photodissociation of gas-phase, closed-shell molecules (see the article by Chuang (1986)). For example, optical excitation of Cl_2 to a dissociative electronic state enables the otherwise non-reactive Cl_2 to efficiently etch S at room temperature (Arikado *et al* 1984).

In the ion/surface-scattering community, it was once believed that the initial charge state of a scattering particle would have no effect on final product distributions. It was argued that efficient charge transfer would lead to an 'equilibration' of charge states near the surface, thus removing any 'memory' of the initial charge state (see Los and Geerlings (1990)). However, van Slooten *et al* (1992) demonstrated that molecules can exhibit distinctly different product branching ratios depending on the charge state of the incident molecule. They showed that H_2^+ incident on Ag(111) dissociates readily via surface neutralization to a repulsive electronic state, whereas neutral H_2 dissociates to a lesser degree via rotational excitation following impact. Schins *et al* (1993) found that excited Rydberg states, H_{2^*}, exhibit dissociation dynamics similar but not identical to those of H_2^+ on the Ag(111) surface. The reason that molecules exhibit memory of the initial charge/electronic state, even though atoms do not, is because motion along vibrational coordinates differs within each electronic state; hence, the evolution of intramolecular motion, which leads to reaction, depends on the exact sequence of electronic transitions (see the article by Gadzuk (1987)).

The majority of surface experiments involving electronically excited species have not utilized gas-phase excitation prior to a molecule's impact with the surface. Instead, an electronic transition within the molecule or substrate has been initiated by electron or photon excitation after the molecule has been adsorbed to the surface. This area of research, termed desorption induced by electronic transitions (DIET), has evolved rapidly in the last decade and is reviewed elsewhere (see *DIET Proceedings* (Tolk *et al* 1983, Brenig and Menzel 1985, Stulen and Knotek 1988, Betz and Vauga 1990, Burns *et al* 1993). The increased importance of plasma processing in the semiconductor industry motivates further investigation into the role of electronic excitation in enhancing molecular reactivity at surfaces (Winters and Coburn 1992).

2.2. *Vibrational energy*

Researchers have pursued three different strategies for measuring the vibrational efficacy of a surface reaction: (i) direct laser excitation of vibrational modes prior to a molecule's impact with a surface: (ii) heated supersonic nozzles for independent control of translational and vibrational energies in the incident molecules; and (iii) detailed balance arguments to relate vibrational-dependent sticking probabilities to state-resolved-desorption experiments.

Direct laser excitation of incident gas-phase molecules has had only moderate success within surface-science applications. Yates *et al* (1979) and Brass *et al* (1970) independently attempted to measure the effect of vibrational excitation on the dissociative chemisorption of CH_4 on Rh. These groups used an HeNe laser to populate the ν_3 and $2\nu_4$ modes of gaseous CH_4 above an Rh surface. Unfortunately, poor sensitivity and low excitation yields prevented either groups from measuring a positive result. Chuang (1981) used a CO_2 laser to vibrationally excite SF_6 prior to its collision with an Si-surface. Adsorption of as many as four infrared photons significantly enhanced the rate of etching and SF_4 product formation. Ulstead *et al* (1980) investigated the reaction of excited NO_2 with C_2H_4 catalysed by a Pt surface. Here, laser excitation of the NO_2 reactants populates the mixed $^2A_1/^2B_1$ electronic system with the majority being in the vibrationally excited electronic ground state, $^2A_1$. A factor of four enhancement in CO_2 production accompanied the introduction of laser radiation to the system. Wittig, Reisler and co-workers collided laser-excited NO_2

with an MgO(100) surface and observed scattered NO fragments (see Ferkel *et al* (1994)). Although the incident molecules were prepared with slightly less internal energy than the dissociation threshold, the impulsive surface collision transferred a sufficient amount of translational energy into rovibrational energy to activate dissociation. This mechanism, termed collision-induced dissociation (CID), occurs via direct inelastic scattering rather than through trapping/desorption.

Laser-pumping experiments experience low overall excitation probabilities; thus, they are susceptible to high background signals arising from the vast majority of unexcited reactants. However, this is not the case for state-selected ion preparation via resonance-enhanced multiphoton ionization (REMPI), because laser-excited ions can be electrostatically separated from unexcited neutrals (see the article by Anderson (1992)). Jacobs and co-workers were the first to apply this novel technique to the burgeoning field of molecular-ion/surface scattering. In the hyperthermal collision-energy regime, Martin *et al* (1992, 1994) found that vibrational energy greatly enhanced the dissociation/two-electron transfer of NO^+ on GaAs(110). Here, state-selected $NO^+(v)$ ions were prepared in vibrational levels ranging from $v = 0$ to 6 and collimated in an ion beam. Figure 4 demonstrates that at 45 eV collision energy, vibrational energy is an order of magnitude more effective than translational energy in promoting scattered O^- products. Jacobs and co-workers argued that neutralization, occurring immediately prior to impact, assisted CID by preparing the incident molecules in a coherent vibrational state, i.e., a state having a restricted distribution of vibrational phases (see the articles by Martin *et al* (1994, 1995)). This effect allowed the initial vibrational energy to add constructively to the translational-to-rovibrational energy transferred upon impact. This study represents the only experimental example of a vibrational enhancement in ion/surface reactions and demonstrates the largest ratio of vibrational to translational efficacies observed in surface science.

A common approach to exploring the effect of vibrational energy on neutral reactive collisions utilizes a heated supersonic nozzle. Raising the nozzle temperature increases the translational energy as well as the internal energy of molecules in the beam; however, by adjusting seeding conditions along with nozzle temperature, one can maintain a constant translational energy while independently varying the vibrational temperature. Rettner *et al* (1985) first demonstrated this approach, and many groups subsequently exploited the technique. It should be noted that rotational motion cools rather efficiently during supersonic expansion and is weakly coupled to the nozzle temperature; therefore, initial rotational energy is frequently ignored in heated-nozzle experiments.

D'Evelyn *et al* (1986) scattered CO_2 on Ni(100) and measured both molecular and dissociative adsorption. Across the translational-energy range of 0.1–1.0 eV, a pronounced vibrational enhancement in the initial sticking probability, S_0, was observed. The authors argue that only the low-lying bending vibrations are excited in the beam. Thus, they suggest that the observed vibrational enhancement supports a bent transition state for the molecule dissociating to CO(a) + O(a) upon collision.

Pfnür *et al* (1986) and Rettner *et al* (1988) examined the sticking of N_2 on W(110) using a heated effusive nozzle. A 10–20% sticking enhancement accompanying the addition of ~0.16 eV of vibrational energy was comparable to the enhancement observed by adding a similar amount of translational energy. Rettner and Stein (1987) compared dissociative sticking measurements at two nozzle temperatures and concluded that vibrational energy is only about half as effective as translational energy in promoting the dissociative chemisorption of N_2 on Fe(111).

Rettner *et al* (1985, 1986) found that CH_4 chemisorption on W(110) is just as enhanced by initial vibrational energy as it is by translational energy. Ceyer and co-workers measured

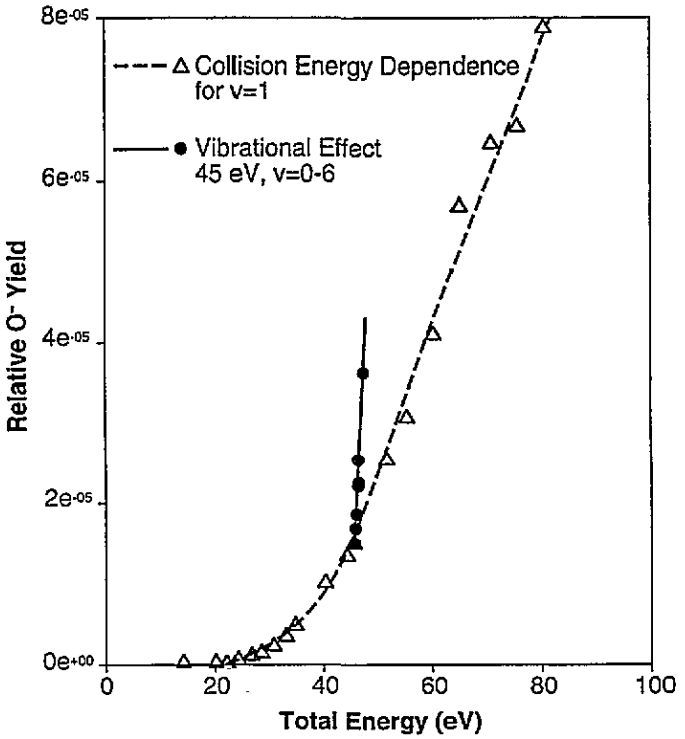

Figure 4. The relative yield of scattered $O^-(^2P)$ from collisions of $NO^+(^1\Sigma^+, v, E_{trans})$ on GaAs(110). The open triangles (dashed curve) were recorded for the $v = 1$ level of incident NO^+ at various collision energies. The closed circles (solid line) show the effect of initial vibrational quanta ($v = 0$–6) at a fixed 45 eV collision energy. (Adapted from the article by Martin *et al* (1994).)

the dissociation probability of CH_4 on Ni(111) as a function of incident translational and vibrational energies (see the article by Lee *et al* (1987)). They found that a modest increase in vibrational energy was at least as, if not more, effective than translational energy in promoting dissociative chemisorption in the translational energy range between 0.5 and 0.7 eV. Moreover, their careful high-resolution electron energy loss spectroscopy (HREELS) analysis demonstrated that dissociative chemisorption of CH_4 results in adsorbed methyl fragments. The authors speculated that the molecule must deform upon impact, thereby moving the H atoms out of the way of the Ni–C attractive interaction. This deformation barrier could be overcome with incident translational energy, initial vibrational energy, or the impact of an inert-gas atom colliding with physisorbed CH_4. Tunnelling of the dissociative H atoms was also implicated from the observed isotope effect. Luntz and Bethune (1989) observed a similar, albeit smaller, vibrational effect in the dissociative chemisorption of CH_4 on Pt(111). In addition, these authors measured an enhanced dissociation with increasing surface temperature that was comparable in efficacy to translational and vibrational energies. Although surface-temperature activation is usually ascribed to a precursor model, Luntz and Harris (1991) argued that, collectively, these three forms of activation are consistent with a direct reaction mechanism involving thermally assisted quantum-mechanical tunnelling. Ukraintsev and Harrison (1994) have proposed an alternative statistical model, which does not include tunnelling but instead recasts the problem into an RRKM formalism.

The model postulates that efficient energy exchange during a direct collision uniformly samples the region of phase space that includes the activated complexes for desorption and dissociation. This treatment provides a remarkable fit to the measured isotope and energetic dependences in scattering, thermal, and photochemical experiments for CH_4Pt(111). An essential presupposition within Ukraintsev and Harrison's model is that all forms of energy contribute equivalently toward activation in the reaction; this condition appears to be valid for CH_4/Pt(111) but is not completely general.

Although the dissociative chemisorption of CH_4 seems universally enhanced by vibrational excitation, McMaster and Madix (1992) found that vibrational energy had no discernible effect on the dissociative sticking probability for C_2H_6 on Pt(111). Larger molecules are more problematic for heated-molecular-beam experiments, because the reagents often dissociate within the nozzle, and because vibrational excitations are distributed over a large number of normal modes.

A simpler prototypical system for determining the role of vibration in sticking is the dissociative chemisorption of H_2 on metals. Hayden and Lamont (1989, 1991) measured the dissociative adsorption probabilities for H_2 and D_2 on Cu(110) as a function of nozzle temperature and seeding conditions. From the seeding data, the authors predicted translational-energy onsets to dissociation for H_2 ($v = 0, 1$) and D_2 ($v = 1, 2$) as a function of the number of initial vibrational quanta. Rendulic and co-workers also observed an enhancement with vibrational energy for H_2, D_2/Cu(111), H_2/Cu(110), H_2/Cu(100), and H_2, D_2/Fe(100) dissociative chemisorption (see the articles by Anger *et al* (1989), Berger *et al* 1990, Berger and Rendulic 1991, Berger *et al* 1992). However, the limited range of beam energies (<0.35 eV) employed in these H_2/Cu studies made it difficult to quantify the relative contributions from the lowest vibrational levels (see the article by Michelsen and Auerbach (1991)). Rettner *et al* (1992) extended the data set to collision energies as high as 0.83 eV for the D_2/Cu(111) system. In this way, they were able to extract the adsorption probability versus energy for D_2 in vibrational states $v = 0$–3.

A complementary study of D_2/Cu(111) exploited REMPI state-resolved detection and the principle of detailed balance (see the article by Michelsen *et al* (1993)). When applied to adsorption/desorption processes, detailed balance requires that, for an equilibrated system, the rate of adsorption be equal to the rate of desorption for any subset of molecules of the equilibrium flux striking the surface (see the articles by Michelsen and Auerbach (1991) or Tully (1994)). Michelsen *et al* (1993) measured the velocity-resolved internal state (v, J) distribution for D_2 formed in recombinative desorption from Cu(111). The authors noted that the velocity distribution from a molecule desorbing in the state (v, J) is equivalent to the product of the flux-weighed velocity distribution at the surface temperature and the adsorption probability function, $S_0(E_i, \theta_i, v, J)$. The latter quantity defines the sticking probability for a molecule approaching the surface with translational energy E_i at an angle of incidence θ_i in vibrational level v and rotational state J. Figure 5 shows the kinetic-energy dependence of the adsorption probability for the first three vibrational levels of D_2 incident on Cu(111). Vibrational energy appears to be 54% as efficacious as translational energy in this system. The measured vibrational populations following Michelsen's permeation/desorption experiment are consistent with those of Kubiak *et al* (1985), who examined the same system but with lower sensitivity.

Schröter *et al* (1987, 1992) performed similar experiments on the recombinative desorption of HD and D_2 from Pd(100); however, these authors measured mean translational energies for the desorbates that were independent of internal-energy state (v, J) and were close to that expected for a thermal distribution at the surface temperature. Although not

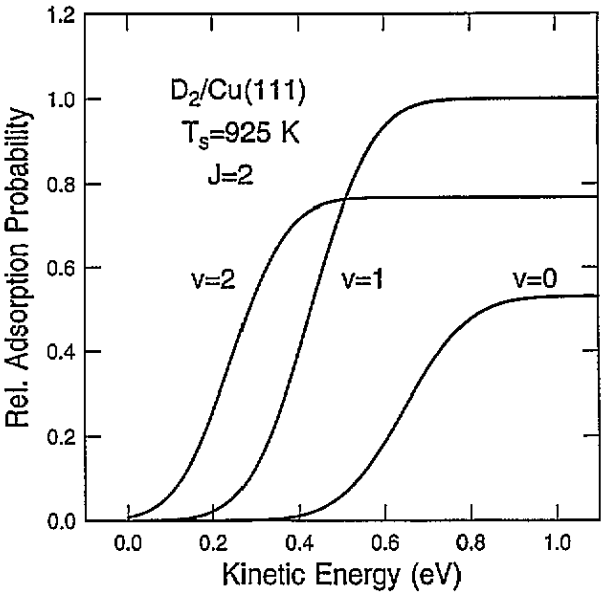

Figure 5. The kinetic-energy dependence of the D_2/Cu(111) adsorption probability. The internal-state-dependent adsorption probability function, $S_0(E_i, \theta_i, v, J)$, is plotted against E_{norm} for three vibrational states ($v = 0$, 1 and 2) bearing a common rotational level ($J = 2$). (From the article by Michelsen *et al* (1993)).

analysed within the same framework as that of Michelsen *et al* (1993), Zacharias' time-of-flight distributions appear to have a depleted low-velocity tail, relative to a Maxwell–Boltzmann distribution at T_s. This is consistent with a low activation barrier (~0.1 eV) to chemisorption. The authors conclude that the coupling between translational and rovibrational degrees of freedom is weak in this system.

A unique approach to assessing the role of vibrational energy in dissociative chemisorption was pursued by Hodgson *et al* (1991, 1992) and Rettner *et al* (1992). Here, a translationally and vibrationally hot molecular beam of D_2 was scattered on a Cu(111) surface. The reflectivity of D_2 in a single rovibrational state ($v = 1$, $J = 4$) after the molecule scattered from the Cu surface was monitored by REMPI. This experiment is sensitive to competing mechanisms for vibrational excitation/depletion. The relative reflectivity of $D_2(v = 1, J = 4)$ takes an abrupt drop at approximately 0.3 eV collision energy, which corresponds to the onset for $v = 1$ dissociative chemisorption. At collision energies approaching 0.6 eV, the relative reflectivity of $D_2(v = 1, J = 4)$ rises above unity, while the corresponding $D_2(v = 0, J = 0, 4)$ level shows a depletion. This latter observation is attributed to molecular vibrational excitation ($v = 0 \rightarrow 1$) traverses a trajectory in which the bond length is extended near the transition state but scatters non-reactively. Rettner and co-workers estimated that the degree of vibrational excitation is roughly equal to the degree of dissociation for collision energies close to the barrier height. In order to avoid ambiguities in assigning the initial state from which the final reflected state originates, Sitz and co-workers have initiated an experimental programme in which stimulated Raman pumping prepares incident H_2 in $v = 1$, $J = 1$. State-selected time-of-flight detection of the same level after molecular scattering from Cu has begun to provide a detailed measure of the transition-state region. Although this set of experiments probes non-reactive collisions, it reveals the stretching motion that H_2 undergoes near the dissociation

barrier on Cu (see the article by Darling and Holloway (1992)).

From this survey of experiments, one concludes that incident vibrational energy is effective in promoting molecule/surface reactions only when a barrier to reaction exists. Analogous to gas-phase dynamics, the reaction probability often demonstrates the greatest vibrational enhancement for the case of a late barrier, where stretching or distortion of a particular bond must occur prior to the molecule reaching the transition state. In some cases, all forms of initial energy exhibit equivalent efficacies, and a statistical model suffices. It has also been observed that electron transfer in conjunction with impulsive energy transfer can give rise to pronounced vibrational dynamics.

2.3. Rotational energy

The effect of rotational motion on surface reaction probability is more difficult to measure, because the density of rotational levels is higher than that of vibrational levels. Supersonic molecular beams do not allow for significant variation of the incident molecule's rotational distribution. Although direct laser preparation of a single rotational level is possible (Misewich *et al* 1985, 1986), a systematic study of the reactivity of rotationally state-prepared molecules at a surface has not yet been undertaken. However, the principal of detailed balance has been successfully exploited to calculate the effect of rotation on sticking. Detailed balance requires state-resolved desorption experiments, which are much simpler to conduct that state-preparative scattering experiments.

As described in subsection 2.2, the dynamics of desorption and adsorption are related for a system under thermal equilibrium or quasiequilibrium. Rotational distributions of molecules undergoing trapping/desorption have been observed for a variety of systems: NO/Ru(001) (Cavanagh and King 1981, King and Cavanagh 1982); NO/Pt(111) (Frenkel *et al* 1981, Asscher *et al* 1982, 1983, Segner *et al* 1983); NO/graphite (Frenkel *et al* 1982, Kuze *et al* 1988); NO/Ge(111) (Mödl *et al* 1985); and NO/Ir(111) (Hamers *et al* 1985, 1988). Although most of these systems demonstrate both direct inelastic scattering and trapping/desorption regimes, these mechanisms can be experimentally distinguished by angular or temporal resolution. In the case of trapping/desorption, the rotational distribution is often well described by a Maxwell–Boltzmann distribution with a temperature lower than the surface temperature. This 'rotational-cooling' effect in desorption has implications on the role of rotational motion in trapping. Through detailed-balance arguments, these results imply that trapping is more hindered for molecules in rotational states with high quantum numbers, J, than it is for those with low J. This is because upon collision with the surface, incident rotational energy generates a translational impulse that impedes trapping when there is no barrier to molecular adsorption. Many reactive systems that undergo dissociative chemisorption show a similar rotational-cooling effect in recombinative desorption experiments, e.g. N_2/Fe (Thorman and Bernasek 1981); D_2/Cu(111) (Kubiak *et al* 1985); OH/Pt(111) (Hsu *et al* 1987, Hsu and Lin 1988); H_2/Pd(100) (Schröter *et al* 1987, 1991); and H_2/Si(100) (Kolasinski *et al* 1991, 1992, Shane *et al* 1992).

However, care must be taken in applying the principle of detailed balance to desorption experiments that only measure a rotational population distribution. Unless the rotationally resolved velocity distribution is explicitly measured for the desorbing molecule, one must assume that final velocity and rotational state are uncorrelated. This approximation is not always justified and can lead to errors in estimating the sticking probability as a function of rotational level. As mentioned in subsection 2.2, Michelsen *et al* (1993) performed an extraordinary set of correlation experiments on the recombinative desorption of D_2 from Cu(111). From these studies, they successfully extracted the sticking probability, $S_0(E_i, \theta_i, v, J)$, as a function of collision energy, incident angle, vibrational level, and

rotational state. The plot of $S_0(E_i, \theta_i, v, J)$ against E_i typically follows an S-shaped curve, characterized in part by a translational-energy threshold, E_0. Figure 6 shows the empirical translational-energy thresholds, E_0, for a variety of rovibrational levels within D_2. These results clearly show that the amount of translational energy needed to surmount the adsorption barrier increases with increasing J for $J < 4$ and decreases with increasing J for $J > 4$. In the high-J limit, rotational energy is approximately 35% as efficacious as translational energy in this system. Making an analogy to gas-phase experiments, the authors argue that rotational motion for low-J states may hinder adsorption by restricting the amount of time the molecule spends in a favourable orientation relative to the surface. At higher values of J, this 'stereodynamic effect' gives way to an 'energy effect', in which rotational energy couples to motion along the reaction coordinate (see the article by Darling and Holloway (1994)). Hence, at high J, increasing the initial number of rotational quanta lowers the translational-energy threshold for reaction.

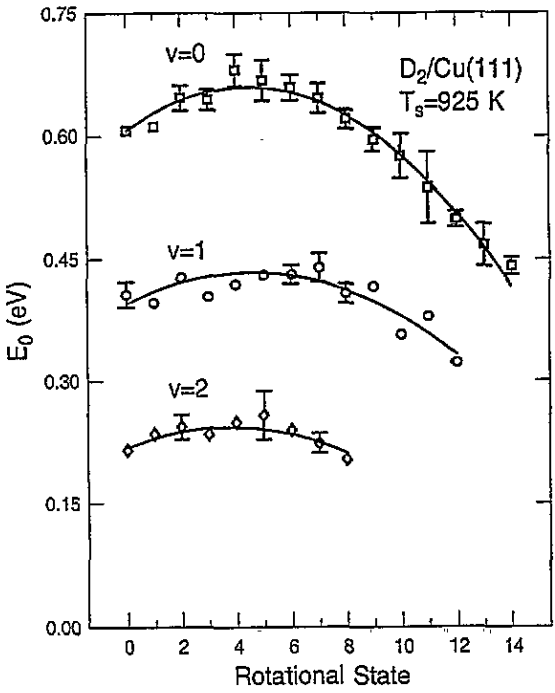

Figure 6. The translational-energy threshold for D_2/Cu(111) dissociative chemisorption as a function of internal (vibrational + rotational) energy. The three clusters of points represent $v = 0$, 1 and 2, while the series of points within each cluster designate individual rotational levels. (From the article by Michelsen *et al* (1993)).

In general, initial rotational energy alters a surface reaction probability only when the operative potential-energy surface has a significant dependence on molecular orientation, i.e., an orientation-dependent well depth, repulsive wall, barrier height, or surface corrugation. The next section explores this issue in greater detail.

3. Approach geometry

3.1. Molecular alignment orientation

Molecular interactions with surfaces are inherently anisotropic, i.e., molecular adsorbates bind with preferential orientations on most surfaces. Thus it is natural to expect that reactive collisions will demonstrate orientational preferences upon approach. This subsection will highlight experiments that probe the effect of an impinging molecule's orientation on reactivity at a surface.

In the absence of external fields, isolated gas-phase molecules have a random distribution of their rotational-angular-momentum vectors as well as their molecular figure axes. However, experimental perturbations may be exploited to create anisotropic vector distributions, quantified in terms of the degree of alignment or orientation associated with the system. Figure 7 illustrates how these two terms are applied to distributions of rotational-angular-momentum vectors or molecular-symmetry-axis directions.

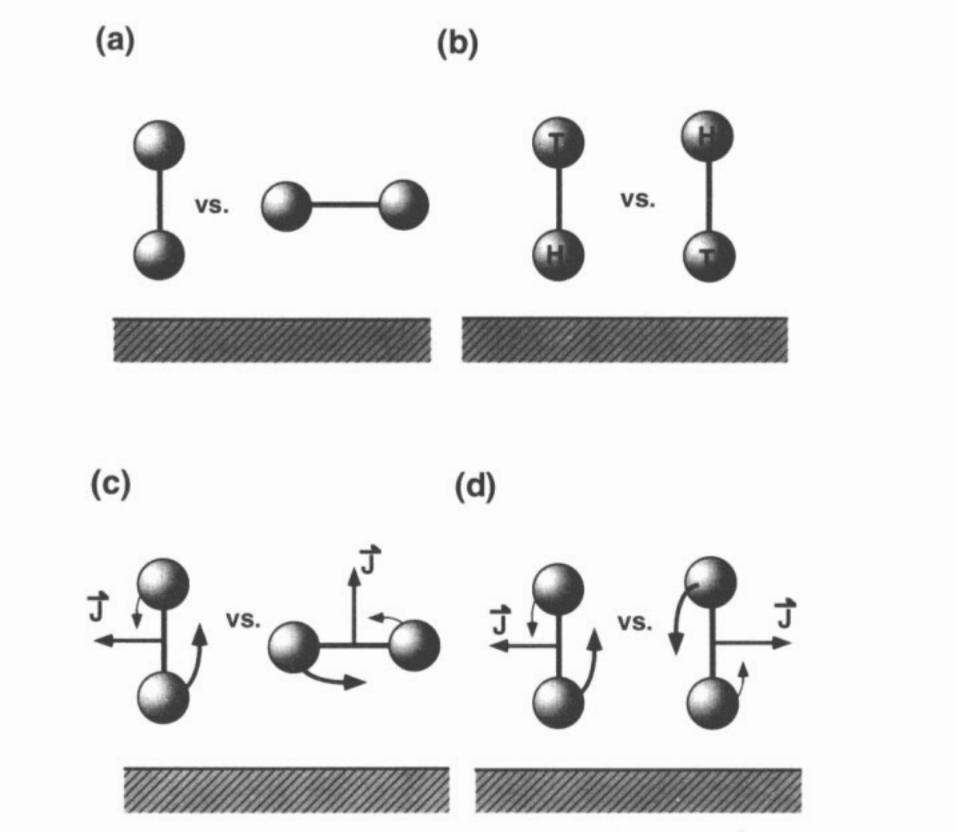

Figure 7. An illustration to clarify the terminology used to describe anisotropic distributions. (a) Alignment of the internuclear axis discriminates between 'end-on' and 'side-on' geometries, whereas (b) orientation of the molecular-symmetry axis specifies a 'heads' versus 'tails' collision. (c) Rotational alignment distinguishes 'cartwheel' from 'helicopter' motion, whereas (d) rotational orientation defines helicity, i.e., clockwise versus anticlockwise rotation.

To continue from the previous discussion involving rotational cooling, the probability that a molecule is trapped at a surface can be inhibited by initial rotational energy.

Furthermore, the direction as well as the magnitude of incident rotational angular momentum may affect the dynamics. Jacobs and co-workers (Jacobs *et al* 1987, 1989, Jacobs and Zane 1989) applied detailed-balance arguments to the state-selective, alignment-sensitive detection of NO desorbing from Pt(111). These experiments revealed that molecules desorbing in rotational levels $J > 12.5$ prefer to rotate in a plane parallel to the surface (helicopter) rather than in a plane perpendicular (cartwheel) to the surface (see figure 7). Consequently, detailed balance suggests that rotationally excited molecules approaching the surface with a cartwheel motion have a lower sticking probability than do molecules approaching with a helicopter motion. This is consistent with the arguments presented in subsection 2.3 for rotational cooling, i.e. trapping is inhibited for cartwheeling molecules, which more efficiently transfer incident rotational energy into a translational thrust away from the surface. Although this study remains the only example of a rotational alignment dependence to trapping/desorption, Hermans (1993) observed similar results for energy relaxation in the scattering of rotationally aligned CH_3F on LiF(001).

Three decades ago Bernstein pioneered a hexapole-electrostatic-field technique (Kramer and Bernstein 1965) for orientating the major symmetry axis of polar molecules. Novakoski and McClelland (1987) first introduced this technique to surface science in the scattering of CHF_3 on Ag(111). Here a hexapole focusing field within the detector measured the molecule's departing orientation upon desorption. In this, as in many other hexapole experiments, orientation effects were characterized by a measured polarization ratio

$$R = \left(I_{\text{heads}} - I_{\text{tails}}\right) \Big/ \left[\left(I_{\text{heads}} + I_{\text{tails}}\right)/2\right] \tag{1}$$

where I_{heads} and I_{tails} represent the scattered molecule intensity corresponding to orientation distributions where the head (−) or tail (+) of the molecule preferentially point toward the surface, respectively. It should be noted that the magnitude of an experimentally determined polarization ratio scales with the average orientation prepared in the incident beam. This latter quantity depends on experimental conditions, e.g., hexapole voltage and purity of rotational states in the focused beam, and as such makes it difficult to compare the magnitude of R measured for different systems. Novakoski and McClelland measured a polarization ratio $R = 0.053 \pm 0.005$ at $T_s = 620$ K, indicating that CHF_3 desorbs with the H preferentially pointing toward the Ag(111) surface. If detailed balance is applicable, this result would suggest that CHF_3 exhibits a greater sticking probability when the H end of the molecule strikes the surface. The observed steric effect underscores the orientation dependence of the molecule/surface potential.

Kleyn, Stolte, and co-workers were the first to apply the hexapole electrostatic technique for orientating molecules incident on a surface (see the articles by Kuipers *et al* (1988, 1989) and Tenner *et al* (1988, 1989a, b, 1991)). They measured the orientation dependence for inelastic scattering and trapping of NO on Ag(111). Trapping exhibits a polarization ratio $R = 0.035$ at $T_s = 600$ K for normal beam energies above 0.02 eV. The preference for trapping when the more repulsive O end of the molecule points toward the surface may arise from the greater amount of translational- to rotational-energy transfer in this configuration. A molecule becomes trapped in the ~0.2 eV adsorption well only when a sufficient amount of initial normal translational energy can be reduced upon collision. In contrast to NO/Ag(111), the adsorption of NO on Pt(111) demonstrates the opposite orientation effect (see the article by Tenner *et al* (1991)). Figure 8 demonstrates that N-end collisions trap more efficiently and hence show less specular scattering than do O-end collisions. The measured steric effect for trapping, $R = -0.025$ (± 0.001) at $T_s = 675$ K, indicates that molecules colliding with

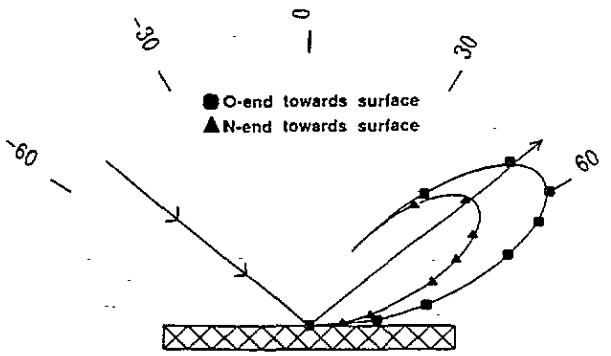

Figure 8. The angular distributions for direct scattering of oriented NO on Pt(111). The incident angle is 50o, the collision energy is 0.180 eV, and the surface temperature is 573 K. Fewer molecules are seen to scatter from the surface when the incident approach is N end first rather than O end first. (From the article by Kuipers *et al* (1989)).

the N atom pointing toward the surface have a higher probability for trapping, presumably because of the stronger chemical bond that Pt makes with N compared to O.

Heinzmann and co-workers have studied the orientation dependence of NO trapping in Ni(100) and Pt(100). In order that their data can be compared to others in this review, (1) will be applied throughout. On Ni(100), sticking exhibits a large polarization ratio, $R = -0.19 \pm 0.02$ at $T_s = 155$ K and normal beam energy, $E_n = 0.125$ eV, for all surface coverages spanning from 0 to 1 monolayer (ML) (see the article by Fecher *et al* (1990a, b)). The coverage-dependent sticking probability implicates an extrinsic precursor to adsorption, i.e., incident molecules colliding with an occupied surface site can temporarily trap and migrate to an empty site. Nevertheless, the data are successfully modelled assuming that the polarization effect arises solely from an orientation preference for those molecules that directly chemisorb. Like the Pt(111) system, NO prefers to chemisorb when the N atom rather than the O atom impacts the Ni(100) surface.

Müller *et al* (1992) explored the stereodynamics of displacing CO with NO on Ni(100) at 160 K. While the adsorption of NO shows a coverage-independent polarization ratio $R = -0.13$ at $T_s = 300$ K and $E_n = 0.107$ eV, the displacement reaction had a complicated polarization ratio. Initially, at high CO coverage the displacement reaction is enhanced when NO approaches O end first ($R = +0.16$); however, as the CO coverage is reduced to $\sim \frac{1}{4}$ ML, displacement is enhanced for N-end collisions ($R = -0.34$).

The dynamics of NO sticking on clean Pt(100) are qualitatively similar to those on clean Ni(100). Across a wide surface-temperature range, 153 K $< T_s <$ 373 K, Müller *et al* (1994a) found that direct chemisorption shows a strong orientation dependence ($-0.58 < R < -0.18$) favouring surface collisions with the N end. Part of the reason why NO adsorption on Pt(111) demonstrates a smaller orientation dependence than it does on Ni(100) and Pt(100) is that the former system has a high sticking probability ($S_0 \geqslant 0.9$); as S_0 nears unity, approach geometry must become inconsequential to sticking.

At higher surface temperatures (393 K), NO reacts with CO-precovered Pt(100) to yield CO_2(g) (see the article by Müller *et al* (1994b)). Figure 9 shows the polarization ratio for CO_2(g) production as a function of exposure time. The authors offer the following explanation for the temporal evolution of the orientational preference. Initially, NO reacts with CO through an Eley–Rideal-type or precursor-mediated (Harris and Kasemo 1981) mechanism. For the CO-saturated surface ($t = 0$ s, $R = -0.6$), N-end collisions are

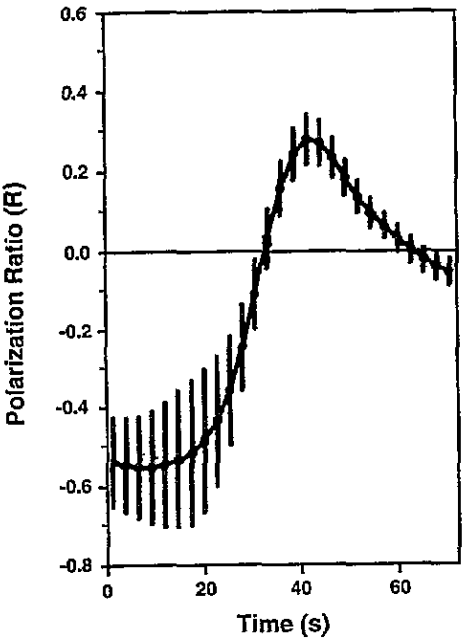

Figure 9. The polarization ratio for CO_2 production on CO-precovered Pt(100) exposed to oriented NO molecules. With increasing exposure time, both the CO coverage and the reaction mechanism change. (*Adapted from the article by Müller et al* (1994b).)

more reactive than O-end collisions. As the reaction proceeds, new adsorption sites become available. Eventually, all the CO adsorbates within the molecular-beam waist are removed by reaction, and diffusion of NO to a CO site along the perimeter recovers the Langmuir–Hinshelwood mechanism. Thus in the asymptotic limit, the reaction polarization ratio reflects only the orientation preference for NO sticking on an NO-covered surface ($R \rightarrow -0.2$); the reaction between NO and CO along the perimeter occurs with no memory of the incident molecule's orientation. In the interim, a positive polarization ratio arises as an artifact of how the data is plotted: a faster reaction rate for N-end collisions depletes the CO coverage more rapidly; thus at $t = 40$ s, the N-end experimental run is well into the Langmuir–Hinshelwood regime, while the O-end run is still reacting with remaining preadsorbed CO through the Eley–Rideal mechanism. If the orientation preference were to be plotted versus CO coverage within the beam waist, the polarization ratio would appear negative everywhere.

Using similar electrostatic orientation techniques, Curtiss and Bernstein (1989) scattered CH_3F on the (0001) face of graphite at 298 K. The specular peak showed a polarization ratio $R = 0.027$, indicating a reduction in the direct scattering probability when the F end of the molecule is oriented towards the surface. Moreover, molecules incident 50° off normal and detected at −10° show a polarization ratio $R = -0.01$; this geometry favours the detection of molecules scattered from the trapping/desorption channel. These two results are consistent with an interpretation that CH_3F may trap more effectively when the F end approaches the surface. Bernstein's group proceeded to measure polarization ratios for over a dozen molecules scattering on graphite (see the article by MacKay *et al* (1989)). Most notably, Mackay *et al* (1990) observed a strong polarization ratio, $R = 0.50$, for specular scattering of CHF_3/graphite. Similar to CH_3F, the polarization ratio flips sign for glancing

incident angles with near normal detection. Consistent with the desorption experiments of Novakoski and McClelland (1987), Bernstein and co-workers speculate that CHF_3 traps preferentially when the H end of the molecule approaches the surface.

Unfortunately, strong electrostatic fields cannot be used to orientate molecular ions; hence, novel approaches have been developed for exploring steric effects in hyperthermal energy ion/surface reactive scattering. Tappe *et al* (1991) scattered H_{2+} on Ni(110) under glancing-incidence conditions and observed the angular distributions of the resulting atomic fragments. They interpreted the asymmetry in these angular distributions to alignment-dependent electron transfer/dissociation dynamics along the incident trajectory.

Snowdon and co-workers carried out an extensive series of glancing-angle scattering experiments using a cation or reneutralized molecular beam (3 keV total energy, 0.7–4.0 eV normal energy). Using coincidence-detection techniques, Rechtien *et al* (1992, 1993), Nesbitt *et al* (1994a, b), and Harder *et al* (1994a, b) measured the final internuclear-axis alignment and kinetic-energy release in the dissociative scattering of H_2^+, D_2^+, N_2^+, and NO^+ on Cu(111). Measurement of the position and arrival time of both fragments in coincidence defines the velocity of the diatom's centre of mass as well as the magnitude and direction of the diatom's relative velocity vector. Dramatically different final internuclear-axis alignments are observed for NO^+ (N_2^+) compared with H_2^+ (D_2^+). For NO^+ (N_2^+), the diatom dissociates with the internuclear axis preferentially directed along the surface normal. Nesbitt *et al* (1994a) speculate that the exit-channel well depth, i.e. attractive N–Cu and O–Cu interactions, minimizes the probability that both fragments will successfully scatter from the surface when the diatom is aligned parallel to the substrate. Conversely, they argue that a molecule aligned along the surface normal has a larger chance for both fragments to reach the detector. Under identical scattering conditions, neutral NO and N_2 exhibit similar internuclear-axis anisotropies as their ionic counterparts. The authors suggest that the similar behaviour occurs because the ion efficiently neutralize on the inward trajectory after which they dissociate by the same mechanism as do the incident neutral molecules.

For the dissociative scattering of H_2^+ (D_2^+), the final internuclear-axis direction preferentially lies parallel to the surface. Unfortunately, this observed alignment bias appears not to be a manifestation of anisotropy within the PES; rather is it a consequence of one fragment losing more energy to the surface than the other (see the article by Harder *et al* (1994b)).

Schins *et al* (1993) utilized a similar experimental approach to explore the dissociative scattering of H_2^+ on Ag(111). Unlike Snowdon and co-workers, Los and co-workers incorporated a detector design that did not restrict the final internuclear-axis direction to lying in the scattering plane. In spite of this experimental improvement, the authors note that tangential energy loss for the incident molecule and scattered fragments necessitates a deconvolution procedure that compromises the ability to extract detailed information from these studies. Nevertheless, the authors implicate direct dissociative neutralization to the lowest dissociative state ($b^3\Sigma_u^+$) of H_2 as the operative mechanism for fragmentation.

Whereas the previous sets of dissociative-scattering experiments were only sensitive to the final alignment of the internuclear axis, Jacobs and co-workers explored *initial* alignment effects in ion/surface reactions. Above collision energies of 20 eV, NO^+ can undergo dissociation and a two-electron transfer on Ag(111) to form O^- products. Greeley *et al* (1994, 1995) utilized $1 + 1'$ REMPI to prepare an aligned distribution of NO^+ ions incident on Ag(111) at collision energies ranging from 35 to 80 eV. Through a Q-branch resonance, plane-polarized light selectively ionized only those molecules with angular momentum vectors, J, aligned parallel to the laser polarization direction. Although the newly formed, state-selected $NO^+(X^1\Sigma, v = 0, J)$ ions rotate freely before colliding with the surface, their

internuclear axis direction is constrained to lie predominantly normal to the laser polarization direction. In this way, the emergence of scattered O^- could be measured for NO^+ molecules that collided predominantly with 'end-on' or alternatively 'side-on' alignments (see figure 7(a)). Figure 10 illustrates that the yield of scattered O^- is enhanced by end-on rather than side-on-type collisions and that this preference diminishes for increasing collision energies. It is improbable that this effect arises from a geometry-dependent electron-transfer probability, because the formation of scattered NO^- appears insensitive to the initial NO^+ alignment. Instead these results, along with corroborating classical trajectory calculations, confirm that CID is the source of the alignment dependence of the reactivity. The impulsive transfer of incident translational energy to rovibrational energy is more effective if the diatom collides with its internuclear axis lying close to the surface normal. This conclusion is consistent with the orientation-dependent rotational rainbows observed for thermal-energy scattering of NO/Ag(111) (see the article by Geuzebroek *et al* (1991)).

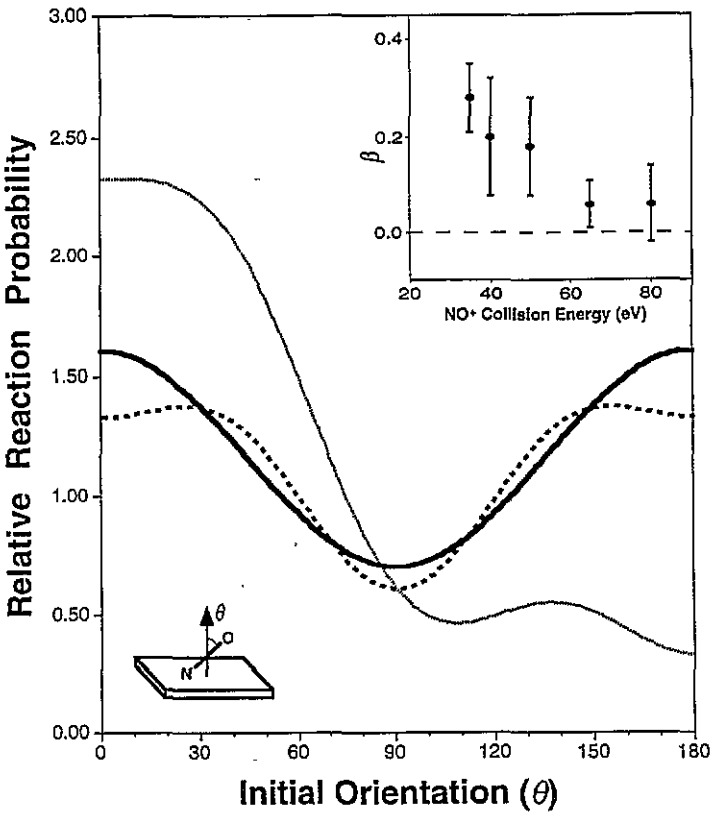

Figure 10. The relative reaction probability for O^- emergence versus the molecular orientation of NO^+ colliding with Ag(111) (35 eV, normal incidence). Only the quadrupole moment of the alignment preference could be determined from the experiment. Each of the three curves is consistent with the measured quadrupole moment ($\beta = 0.3$ at 35 eV) and they demonstrate that near-end on collisions are at least twice as reactive as side-on collisions. The inset shows the dependence of the quadrupole moment on collision energy, where $\beta = 0$ represents no alignment preference. (Adapted from the article by Greeley *et al* (1994).)

The experiments reviewed in this section provide wonderful examples of the interesting geometric constraints in molecule/surface reactions. Furthermore, they complement the

wealth of structural information obtained for molecules adsorbed on a variety of surfaces. It is hoped that a relationship between equilibrium bonding geometries and the most favourable approach geometry for reactions can be firmly established.

3.2. The surface impact parameter

Determination of the chemisorption sites for molecular adsorbates is a first step to establishing catalytic reaction mechanisms; this is commonly achieved through a battery of complementary surface-sensitive spectroscopies, i.e. low-energy electron diffraction (LEED), high-resolution electron energy-loss spectroscopy (HREELS), infrared absorption spectroscopy (IRAS), x-ray absorption fine structure (XAFS), electron-stimulated-desorption ion angular distributions (ESDIAD), time-of-flight scattering and recoiling spectroscopy (TOFSARS), scanning tunnelling microscopy (STM), etc. However, a more difficult question to address is how the impact site of an impinging gas-phase molecule determines the molecule's subsequent reactivity at a surface. This question may be asked of a variety of surface processes: trapping, chemisorption, electron transfer, dissociative scattering, sputtering, etching, addition reactions, etc.

Analogous to the terminology applied to individual gas-phase reactive trajectories, we define the surface impact parameter as the point on the surface at which the incident molecule's centre of mass would collide in the absence of any molecule/surface interactions. The effect that a molecule's surface impact parameter has on reaction probability can be inconsequential for some reaction mechanisms. For example, in a Langmuir–Hinshelwood mechanism, reactants first chemisorb or physisorb to the surface; next one or both reagents diffuse along the surface; after two energetically and sterically suitable reactants encounter one another, they form products; finally, the product molecules desorb from the surface. Here, the surface impact parameter may only affect the initial trapping probability and not the reaction probability between adsorbates. In contrast, an Eley–Rideal mechanism involves a direct reactive collision between an impinging gas-phase molecule and an adsorbate. In this case, the surface impact parameter might have a pronounced effect on the reaction probability. Hence, determining the relationship between reaction probability and surface impact parameter provides important mechanistic information.

Unfortunately, it is impossible to focus with atomic precision a beam of incident molecules, so as to directly control their surface impact parameter. Instead, all surface impact parameters are sampled statistically within a given experimental measurement. Variation of the molecular beam's incident angle relative to the surface normal can restrict the distribution of sampled surface impact parameters; however, this also alters the normal incident energy, which in itself can exert a pronounced effect on reactivity.

Classical trajectory simulations have demonstrated that the surface impact parameter plays an important role in energy transfer during surface collisions (see the articles by Alexander (1991), Masson *et al* (1994), and Pouilly *et al* (1994)). Moreover, trapping can be enhanced for surface impact parameters where incident momentum directed along the surface normal is converted into tangential momentum (see the articles by Tully (1980) and Jacobs and Zare (1989)). Unfortunately, the validity of these principles can only be summarised indirectly from experiments.

A powerful experimental probe of the site dependence of the reactivity is realized by the angle- and energy-resolved detection of scattered/desorbed product molecules. Matsushima *et al* (1993a, b) and Ohno *et al* (1993) exploited this principle in the recombinative desorption of CO_2 on Ir(110)(1 × 2), Pd(110), Pt(110)(1 × 2), and Pt(112). In each case, CO and O were coadsorbed at a fraction of a monolayer. As the surface was heated, the velocity distribution of CO_2 was measured for various polar and azimuthal angles. In

summary, the product velocity distribution can be fitted to a temperature five times that of the surface. Moreover, the angular distribution is sharply peaked and non-cylindrically symmetric about the surface normal. Matsushima and co-workers propose that O adatoms are tightly bound at high-coordination sites. The CO adsorbates diffuse to and react with the stationary O atoms. The nascent CO_2 is only weakly bound; moreover, it is born on a repulsive region of the CO_2/surface potential due to the initially short O/surface bond length. Analogous to ESDIAD, the authors argue that prompt CO_2 desorption from this repulsive potential will lead to a product angular distribution with the same symmetry as the desorption site. Applying a simple hindered translational-energy model to fit the angular-distribution data, the researchers implicate the sites from which the CO_2 products are ejected. Although higher coverages increase the product translational energy and sharpen the angular distributions, the nature of the reaction site is believed to be invariant with coverage. Applying detailed balance to this system, one would predict that dissociative chemisorption of CO_2 is translationally activated and proceeds at the same sites (surface impact parameters) implicated from the desorption experiments.

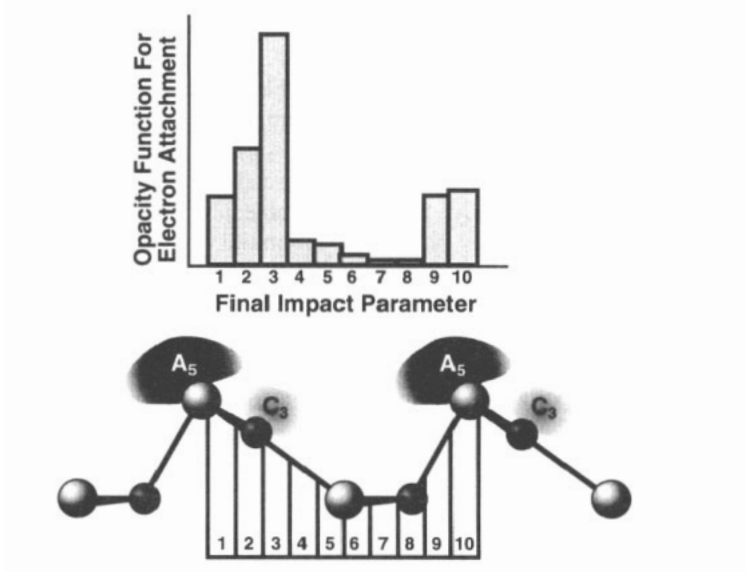

Figure 11. The opacity function for electron attachment to form O^- in the scattering of NO^+ on GaAs(110). The bar plot represents the probability that an electron from the surface will attach to the emerging O fragment as a function of the final surface impact parameter. The charge densities for the C_3 and A_5 dangling-bond states are illustrated above the lattice. (From the article by Morris *et al* (1995).)

Morris *et al* (1995) explored the surface-impact-parameter dependence of dissociative scattering of NO^+ on GaAs(110). The (110) face of GaAs is characterized by rows and troughs, where Ga and As atoms are situated opposite one another (see figure 11). As a result, the surface lacks a reflection plane parallel to the rows. With state-selected $NO^+(v = 1)$ incident along the surface normal, the flux of O^- products was recorded in a scattering plane perpendicular to the rows and troughs. Here it was observed that O^- products preferentially emerge to one side rather than the other side of the surface normal. To address whether this apparent scattering asymmetry arises solely from the

surface corrugation, classical trajectory simulations were performed on a 105 atom slab. Surprisingly, the classical trajectory model predicts an asymmetry in the opposite direction. Consequently, Jacobs and co-workers introduced a surface opacity function for electron attachment, expressing the probability that an electron from the surface will attach to the dissociating diatom, as a function of the O atom's last point of impact at the surface (final surface impact parameter). By fitting the model's predicted angular distribution with that measured from experiment, a surface opacity function for electron attachment was extracted. This function, shown in figure 11, clearly indicates that O^- emerges only if it last scatters from the peaks of the GaAs rows. Of particular importance, the C_3 and A_5 surface states correspond to dangling bonds on the Ga- and As-row atoms, respectively. These surface states, being close to the Fermi level, are near-resonant with the impacted O atom's affinity level. Thus, a plausible explanation for the observed scattering asymmetry is that O^- products emerge only after the O fragment achieves sufficient spatial overlap, with the C_3 or A_5 surface states, to attach an electron. The notion of a surface-impact-parameter dependence for charge transfer is not unprecedented. In atomic-ion scattering, Geerlings *et al* (1987), Kimmel *et al* (1991), German *et al* (1993), and Hsu *et al* (1993) have observed a relationship between surface impact parameter and electron-transfer probability. However, the NO^+/GaAs(110) system remains the only molecular-ion scattering system for which a relationship between final surface impact parameter and reaction probability has been established.

4. Conclusions

This review has demonstrated the merits of investigating molecule/surface reactions with attention to energetic and geometric considerations. Specifically, the reaction probability for a molecule incident on a surface depends on both the initial energy (electronic, translational, vibrational, and rotational) and the molecule's approach geometry (spatial orientation and surface impact parameter). In most cases, translational energy is found to be equally or more efficacious than vibrational or rotational energies in promoting dissociation, with NO^+/GaAs(110) being a notable exception. Experiments reveal that molecular orientation can have a pronounced effect on surface reactivity, because of strongly directional covalent interactions as well as geometric dependences in the energy-transfer dynamics. The incident and final surface impact parameters are seen to be important to Eley–Rideal and electron-transfer reactions, respectively. Together with model simulations, the reviewed scattering experiments provide salient details on the characteristic atomic motions associated with prototypical surface reactions.

Acknowledgments

Scott Martin, Neil Greeley, and John Morris are thanked for their careful reading of this manuscript. The author gratefully acknowledges the Alfred P Sloan Foundation and the National Science Foundation for their support of his work in this area.

References

Alexander J H 1991 *J. Chem. Phys.* **94** 8486
Anderson S L 1992 *Adv. Chem. Phys.* **82** 177

Anger G, Winkler A and Rendulic K D 1989 *Surf. Sci.* **200** 1
Arikado T, Sekine M, Okano H and Horiike Y 1984 *Mater. Res. Soc. Symp. Proc.* vol 29 (Pittsburgh, PA: Materials Research Society) p 167
Asscher M, Guthrie W, Lin T and Somorjai G 1982 *Phys. Rev. Lett.* **49** 76
—— 1983 *J. Chem. Phys.* **78** 6992
Berger H F, Grösslinger E and Rendulic K D 1992 *Surf. Sci.* **261** 313
Berger H F, Leisch M, Winkler A and Rendulic K D 1990 *Chem. Phys. Lett.* **175** 425
Berger H F and Rendulic K D 1991 *Surf. Sci.* **253** 325
Betz G and Varga P (ed) 1990 *DIET-IV (Springer Series in Surface Sciences 19)* (Berlin: Springer)
Brass S G, Reed D A and Ehrlich G 1979 *J. Chem. Phys.* **70** 5244
Brenig W and Menzel D (ed) 1985 *DIET-II (Springer Series in Surface Sciences 4)* (Berlin: Springer)
Burns A, Jennison D and Stechel E B (ed) 1993 *DIET-V (Springer Series in Surface Science 31)* (Berlin: Springer)
Cavanagh R R and King D S 1981 *Phys. Rev. Lett.* **47** 1829
Ceyer S T 1988 *Ann. Rev. Phys. Chem.* **39** 479
Chuang T J 1981 *J. Chem. Phys.* **74** 1453
—— 1986 *Surf. Sci.* **178** 763
Curtiss T J and Bernstein R B 1989 *Chem. Phys. Lett.* **161** 212
Darling G R and Holloway 1992 *J. Chem. Phys.* **97** 734
—— 1994 *J. Chem. Phys.* **101** 3268
D'Evelyn M P, Hamza A V, Gdowski G E and Madix R H 1986 *Surf. Sci.* **167** 451
Fecher G H, Böwering N, Volkner M, Pawlitzky B and Heinzmann U 1990a *Surf. Sci.* **230** L169
Fecher G H, Volkner M, Pawlitzky B, Böwering N and Heinzmann U 1990b *Vacuum* **41** 265
Ferkel H, Singleton J T, Reisler H and Wittig C 1994 *Chem. Phys. Lett.* **221** 447
Frenkel F, Häger J, Krieger W, Walther H, Campbell C, Ertl G, Kuipers H and Segner J 1981 *Phys. Rev. Lett.* **46** 152
Frenkel F, Häger J, Krieger W, Walther H, Ertl G, Wegner J and Vielhaber W 1982 *Chem. Phys. Lett.* **90** 225
Gadzuk J W 1987 *Chem. Phys. Lett.* **136** 402
Geerlings J J C, Kwakman L F T and Los J 1987 *Surf. Sci.* **184** 305
German K A H, Weare C B, Varekamp P R, Andersen J N and Yarmoff J A 1993 *Phys. Rev. Lett.* **70** 3510
Geuzebroek F H, Wiskerke A E, Tenner M G, Kleyn A W, Stolte S and Namiki A 1991 *J. Phys. Chem.* **95** 8409
Greeley J N, Martin J S, Morris J R and Jacobs D C 1994 *Surf. Sci.* **83** 6045
Greeley J N, Martin J S, Morris J R and Jacobs D C 1995 *J. Chem. Phys.* submitted
Hamers R J, Houston P L and Merrill R P 1985 *J. Chem. Phys.* **83** 6045
—— 1988 *J. Chem. Phys.* **88** 6548
Harder R, Nesbitt A, Golichowski A, Herrman G and Snowdon K J 1994a *Surf. Sci.* **316** 47
—— 1994b *Surf. Sci.* **316** 63
Harris J and Kasemo B 1981 *Surf. Sci. Lett.* **105** L281
Hayden B E and Lamont C L A 1989 *Phys. Rev. Lett.* **63** 1823
—— 1991 *Surf. Sci.* **243** 31
Hermans L J F 1993 *Comment. At. Mol. Phys.* **29** 229
Hodgson A, Moryl J, Traversaro P and Zhao H 1992 *Nature* **356** 501
Hodgson A, Moryl J and Zhao H 1991 *Chem. Phys. Lett.* **182** 152
Hsu C C, Bousetta A, Rabalais J W and Nordlander P 1993 *Phys. Rev.* B **47** 2369
Hsu D S Y, Hoffbauer M A and Lin M C 1987 *Surf. Sci.* **194** 25
Hsu D S Y and Lin M C 1988 *J. Chem. Phys.* **88** 432
Jacobs D C, Kolasinski K W, Madix R J and Zare R N 1987 *J. Chem. Phys.* **87** 5038
Jacobs D C, Kolasinski K W, Shane S F and Zare R N 1989 *J. Chem. Phys.* **91** 3182
Jacobs D C and Zare R N 1989 *J. Chem. Phys.* **91** 3196
Kimmel G A, Goodstein D M, Levine Z H and Cooper B H 1991 *Phys. Rev.* B **43** 9403
King D S and Cavanagh R R 1982 *J. Chem. Phys.* **76** 5634
Kolasinski K W, Shane S F and Zare R N 1991 *J. Chem. Phys.* **95** 5482
—— 1992 *J. Chem. Phys.* **96** 3995
Kramer K H and Bernstein R B 1965 *J. Chem. Phys.* **42** 676
Kubiak G D, Sitz G O and Zare R N 1985 *J. Chem. Phys.* **83** 2538
Kuipers E W, Tenner M G, Kleyn A W and Stolte S 1988 *Nature* **334** 420
—— 1989 *Phys. Rev. Lett.* **62** 2152
Kuze H, Häger J and Walther H 1988 *Chem. Phys. Lett.* **153** 569
Lee M B, Yang Q Y and Ceyer S T 1987 *J. Chem. Phys.* **87** 2724

Levine R D and Bernstein R B 1987 *Molecular Reaction Dynamics and Chemical Reactivity* (Oxford: Oxford University Press)
Los J and Geerlings J J C 1990 *Phys. Rep.* **190** 133
Luntz A C and Bethune D S 1989 *J. Chem. Phys.* **90** 1274
Luntz A C and Harris J 1991 *Surf. Sci.* **258** 397
Mackay R S, Curtiss T J and Bernstein R B 1989 *Chem. Phys. Lett.* **164** 341
—— 1990 *J. Chem. Phys.* **90** 801
Martin J S, Feranchak B T, Morris J R, Greeley J N and Jacobs D C 1995 *J. Phys. Chem.* submitted
Martin J S, Greeley J N, Morris J R, Feranchak B T and Jacobs D C 1994 *J. Chem. Phys.* **100** 6781
Martin J S, Greeley J N, Morris J R and Jacobs D C 1992 *J. Chem. Phys.* **97** 9476
Masson D P, Hanisco T F, Nichols W L, Yan C, Kummel A C and Tully J C 1994 *J. Chem. Phys.* **101** 3341
Matsushima T, Ohno Y and Rar A 1993a *Surf. Sci.* **293** 145
Matsushima T, Shobatake K and Ohno Y 1993b *Surf. Sci.* **283** 101
McMaster M C and Madix R J 1992 *Surf. Sci.* **275** 265
Michelsen H A and Auerbach D J 1991 *J. Chem. Phys.* **94** 7502
Michelsen H A, Rettner C T, Auerbach D J and Zare R N 1993 *J. Chem. Phys.* **98** 8294
Misewich J, Roland P A and Loy M M T 1986 *Surf. Sci.* **171** 483
Misewich J, Zacharias H and Loy M M T 1985 *Phys. Rev. Lett.* **55** 1919
Mödl A, Robota H, Segner J, Vielhaber W, Lin M and Ertl G 1985 *J. Chem. Phys.* **83** 4800
Morris J R, Martin J S, Greeley J N and Jacobs D C 1995 *Surf. Sci.* at press
Müller H, Dierks B, Hamza F, Zagatta G, Fecher G H, Böwering N and Heinzmann U 1992 *Surf. Sci.* **269/270** 207
Müller H, Zagatta G, Böwering N and Heinzmann U 1994a *Chem. Phys. Lett.* **223** 197
Müller H, Zagatta G, Brandt M, Wehmeyer, Böwering N and Heinzmann U 1994b *Surf. Sci.* **307–309** 159
Nesbitt A, Harder R, Golichowski A, Herrmann G and Snowdon K J 1994a *Surf. Sci.* **307–309** 147
—— 1994b *Chem. Phys.* **179** 215
Novakoski L V and McClelland G M 1987 *Phys. Rev. Lett.* **59** 1259
Ohno Y, Matsushima T and Miki H 1993 *Surf. Sci.* **281** 234
Pfnür H E, Rettner C T, Auerbach D J, Madix R J and Lee J 1986 *J. Chem. Phys.* **85** 7452
Pouilly G, Robbe J-M and Lemoine D 1994 *J. Phys.: Condens. Matter* **45** 9689
Rechtien J-H, Harder R, Herrmann G, Nesbitt A, Tellioglu K and Snowdon K J 1993 *Surf. Sci.* **282** 137
Rechtien J-H, Harder R, Herrmann G and Snowdon K J 1992 *Surf. Sci.* **272** 240
Rettner C T, Auerbach D J and Michelsen H A 1992 *Phys. Rev. Lett.* **68** 2547
Rettner C T, Pfnür H E and Auerbach D J 1985 *Phys. Rev. Lett.* **54** 2716
—— 1986 *J. Chem. Phys.* **84** 4163
Rettner C T, Pfnür H E, Stein H and Auerbach D J 1988 *J. Vac. Sci. Technol.* **6** 899
Rettner C T and Stein H 1987 *J. Chem. Phys.* **87** 770
Schins J M, Vrijen R B, van der Zande W J and Los J 1993 *Surf. Sci.* **280** 145
Schröter L, Ahler G, Zacharias H and David R 1987 *J. Electron Spectrosc. Relat. Phenom.* **45** 403
Schröter L, David R and Zacharias H 1991 *Surf. Sci.* **258** 259
Schröter L, Trame C, David R and Zacharias H 1992 *Surf. Sci.* **272** 229
Segner J, Robota H, Vielhaber W, Ertl G, Frenkel F, Häger J, Krieger W and Walther H 1983 *Surf. Sci.* **131** 273
Shane S F, Kolasinski K W and Zare R N 1992 *J. Chem. Phys.* **97** 1520
Stulen R H and Knotek M L (ed) 1988 *DIET-III (Springer Series in Surface Sciences 13)* (Berlin: Springer)
Tappe W, Niehop A, Schmidt K and Heiland W 1991 *Europhys. Lett.* **15** 405
Tenner M G, Kuipers E W, Kleyn A W and Stolte S 1988 *J. Chem. Phys.* **89** 6552
—— 1989a *Surf. Sci.* **211/212** 819
—— 1989b *Chem. Phys.* **138** 451
—— 1991 *J. Chem. Phys.* **94** 5197
Thorman R P and Bernasek S L 1981 *J. Chem. Phys.* **74** 6498
Tolk N H, Traum M M, Tully J C and Madey T E (ed) 1983 *Desorption Induced by Electronic Transitions, DIET-I (Springer Series in Chemical Physics 24)* (Berlin: Springer)
Tully J C 1980 *J. Chem. Phys.* **73** 1975
—— 1994 *Surf. Sci.* **299/300** 667
Ukraintsev V A and Harrison I 1994 *J. Chem. Phys.* **101** 1564
Ulstead M E, Talley L D, Trevault D E and Lin M C 1980 *Opt. Eng.* **19** 94
van Slooten U, Andersson D R, Kleyn A W and Gislason E A 1992 *Surf. Sci.* **274** 1
Winters H F and Coburn J W 1992 *Surf. Sci. Rep.* **14** 161
Yates J T, Zinck J J, Sheard S and Weinberg W H 1979 *J. Chem. Phys.* **70** 2266